

Width of the QCD transition in a Polyakov-loop DSE model

D. Horvatić,^{1,2} D. Blaschke,^{3,4} D. Klabučar,¹ and O. Kaczmarek⁵

¹*Physics Department, Faculty of Science, University of Zagreb, Zagreb 10000, Croatia*

²*Institut für Physik, Karl-Franzens-Universität Graz, A-8010 Graz, Austria*

³*Institute for Theoretical Physics, University of Wrocław, 50-204 Wrocław, Poland*

⁴*Bogoliubov Laboratory of Theoretical Physics, JINR Dubna, 141980 Dubna, Russia*

⁵*Department of Physics, Bielefeld University, D-33501 Bielefeld, Germany*

(Dated: March 27, 2018)

We consider the pseudocritical temperatures for the chiral and deconfinement transitions within a Polyakov-loop Dyson-Schwinger equation approach which employs a nonlocal rank-2 separable model for the effective gluon propagator. These pseudocritical temperatures differ by a factor of two when the quark and gluon sectors are considered separately, but get synchronized and become coincident when their coupling is switched on. The coupling of the Polyakov-loop to the chiral quark dynamics narrows the temperature region of the QCD transition in which chiral symmetry and deconfinement is established. We investigate the effect of rescaling the parameter T_0 in the Polyakov-loop potential on the QCD transition for both the logarithmic and polynomial forms of the potential. While the critical temperatures vary in a similar way, the width of the transition is stronger affected for the logarithmic potential. For this potential the character of the transition changes from crossover to a first order one when $T_0 < 210$ MeV, but it remains crossover in the whole range of relevant T_0 values for the polynomial form.

PACS numbers: 11.10.Wx,12.38.Aw,12.38.Mh,12.39.Fe

I. INTRODUCTION

The QCD phase transition between highly excited hadronic matter and the quark-gluon plasma is presently under experimental investigation at ultra-relativistic heavy-ion collider facilities like the Relativistic Heavy-Ion Collider (RHIC) at the Brookhaven National Laboratory or the Large Hadron Collider (LHC) at CERN Geneva. Its theoretical description requires methods to solve QCD at finite temperature in the highly nonperturbative low-energy domain. At present, the only method to obtain ab-initio solutions of QCD in this domain is lattice QCD (LQCD).

LQCD calculations are becoming available in the region of physical quark masses [1–8] and allow for a quantitative description of the equation of state (EoS) and a determination of the pseudocritical temperature. Although still afflicted with some uncertainty, those results can be used in phenomenological studies of the QCD transition relevant for current and future heavy ion experiments at RHIC and LHC. Hadron gas model calculations give a good description of the EoS in the confined phase. Furthermore, statistical models of hadron production [9, 10] can be used to extract the chemical freeze-out temperature which serves as a lower limit for the deconfinement temperature.

Even so, there are limitations to explore the full QCD phase diagram with LQCD. Hence dynamical models for the phase structure of QCD which can be calibrated with hadron phenomenology and with finite- T LQCD remain an important tool. Particularly useful are chiral quark models of the Nambu–Jona-Lasinio (NJL)-type [11–16], but they suffer from nonphysical quark excitations at low temperatures, below T_c . Also the contribution from

the gluon sector to the thermodynamics is missing. A rather successful generalization has recently been suggested which fixes both these problems by coupling the chiral dynamics of the quark sector as modeled within the NJL model to a mean-field description of the gluon sector with an effective potential as a function of the Polyakov-loop (PL) variable, fitted to the pure gauge lattice simulations for the Yang-Mills pressure [17]. Within such a PNJL model [18–20], a remarkable agreement with other LQCD results as, e.g., for the chiral susceptibilities, could be achieved once the temperature in the fit of the gluon mean-field is appropriately scaled to the critical temperature obtained in the lattice simulations [17, 21, 22]. The success of this type of chiral quark model in reproducing features of lattice QCD simulations has led to a number of applications as well as to extensions of the model. For example, we would like to mention here the extensions to include eight-quark interactions [23] and to consider a coupling (entanglement) between the scalar coupling constant and the Polyakov-loop [24].

The deficiency of such a PNJL model is in the poor quark dynamics with, e.g., a constant, momentum independent quark mass function. Although the excitation of quark degrees of freedom is strongly suppressed at low temperatures by the destructive interference due the PL phase factors, a dynamical confinement mechanism is absent. In order to improve the quark dynamics of a PNJL model, the local current-current form of the quark interaction has been generalized to a nonlocal one [25–27]. In this way, a dynamical quark mass function can be modeled using appropriate covariant *ansätze* for the form factor of the nonlocality. However, before a quantitative comparison with quark mass functions measured in LQCD (see, e.g., Ref. [28]) can be made, one has also

to introduce a nonlocal dynamical modification of the Dirac vector part of the quark propagator for describing the quark wave function renormalization as was recently accomplished within the nonlocal PNJL model in Refs. [29, 30].

Alternatively, one can start from QCD Dyson-Schwinger equations (DSEs), apply a symmetry-preserving truncation scheme, and solve the resulting equations for the Schwinger functions. In the recent years, this approach has reached a new level of maturity (see, e.g., Refs. [31–33] for reviews). This ongoing progress in DSEs also includes *ab initio* type of calculations [34, 35] pertaining to PL and related to other functional approaches.

There are attempts to derive nonlocal PNJL or PDSE models as a low-energy limit of QCD [36], which used insights that have been obtained in the functional renormalization group method [37, 38]. Functional methods also suggest close relation between the chiral and the confinement transition [38, 39], and even the relation of both of them with the $U_A(1)$ symmetry restoration [40]. These studies are worth a systematic further development.

Since QCD applications at $T > 0$ are in general considerably more difficult than at $T = 0$, it is often useful to take a more phenomenological approach: one chooses a suitable (e.g., phenomenologically successful) effective dressed-gluon propagator model and solves the resulting $T > 0$ DSEs for the Schwinger functions in the quark sector [32]. Such an approach has many advantages over NJL-type models as, e.g., a dynamical confinement mechanism. However, as has been analyzed in [41] the critical temperatures obtained within such non-perturbative low-energy QCD models turn out to be too low when compared with LQCD results.

In the present work we suggest that this shortcoming might have its origin in residual color correlations and we investigate a generalization where the PL is coupled to the quark sector DSE (PDSE). For the purpose of this exploratory approach, we will restrict ourselves in this PDSE model to a rank-2 separable form of the effective gluon propagator [42] which at the rainbow-ladder level of truncation is equivalent to a full DSE model with translation-invariant gluon propagator once the model form factors of the interaction are chosen appropriately [43]. For the time being one may take the pragmatic approach of modeling form factors of the rank-2 separable interaction such that both, the dynamical quark mass function and the wave function renormalization as measured in LQCD at zero temperature can be repro-

duced to high accuracy. With an interaction model fixed in this way, the approach developed here can be used to predict thermodynamics and hadron properties of low-energy QCD at finite temperature, calibrate the results with LQCD and extend the approach subsequently to the whole QCD phase diagram, i.e., into regions presently inaccessible to LQCD.

In the present work, by analyzing the temperature behavior of the order parameters in the model, the dynamically generated light and strange quark masses as well as the PL variable, we find that the critical temperatures for the chiral and the deconfinement transitions measured by the peaks in the corresponding susceptibilities (defined here as the temperature derivatives of the order parameters) coincide at the per mille level of accuracy. We will discuss the effect of rescaling the critical temperature parameter T_0 of the PL potential [44–47] once applications with a finite number of quark flavors and a possible chemical potential are considered and how this affects the width of the QCD transition region.

As a possible application of this class of models we discuss the temperature dependence of scalar and pseudoscalar meson properties at finite temperatures towards the chiral symmetry restoration. We devote special attention to the investigation of a Gell-Mann–Oakes–Renner (GMOR)-like relationship for the mass of pseudoscalar mesons at finite temperatures. We find that the GMOR-like relation proves to be robust up to the critical temperature, as a manifestation of the implemented confinement mechanism at the rainbow-ladder level of the description, where the coupling to the PL provides a very effective suppression of the quark degrees of freedom in the medium which otherwise induce a medium dependence which is unphysical below T_c . In this regime, medium effects have to be absent as long as hadronic excitations in the medium are disregarded.

II. SEPARABLE PDSE MODEL

A. Thermodynamical potential and order parameters

The central quantity for the analysis of the thermodynamical behavior is the thermodynamical potential which in the PDSE approach is a straightforward generalization of the standard CJT functional [48, 49]

$$\Omega(T) = -T \ln Z(T) = \mathcal{U}(\Phi, \bar{\Phi}) - T \text{Tr}_{\vec{p}, n, \alpha, f, D} \left[\ln \{ S_f^{-1}(p_n^\alpha, T) \} - \Sigma_f(p_n^\alpha, T) \cdot S_f(p_n^\alpha, T) \right], \quad (1)$$

where the full quark propagator for the flavor $f = u, d, s$,

$$\begin{aligned} S_f^{-1}(p_n^\alpha, T) &= S_{f,0}^{-1}(p_n^\alpha, T) + \Sigma_f(p_n^\alpha, T) \\ &= i\vec{\gamma} \cdot \vec{p} A_f((p_n^\alpha)^2, T) \\ &\quad + i\gamma_4 \omega_n C_f((p_n^\alpha)^2, T) + B_f((p_n^\alpha)^2, T) \end{aligned} \quad (2)$$

is defined by the DSE for the quark self-energy Σ , see below. The Polyakov-loop potential is first taken in the

form [50]

$$\frac{\mathcal{U}_{\log}(\Phi, \bar{\Phi})}{T^4} = -\frac{1}{2}a(T)\bar{\Phi}\Phi + b(T) \ln [1 - 6\bar{\Phi}\Phi + 4(\bar{\Phi}^3 + \Phi^3) - 3(\bar{\Phi}\Phi)^2] \quad (3)$$

with $a(T) = a_0 + a_1(T_0/T) + a_2(T_0/T)^2$, $b(T) = b_3(T_0/T)^3$. The corresponding parameters are taken from Ref. [50], $a_0 = 3.51$, $a_1 = -2.47$, $a_2 = 15.22$ and $b_3 = -1.75$ where they have been adjusted to fit the pressure obtained in lattice gauge theory simulations of SU(3) Yang-Mills theory. In most of the literature on the PNJL model, the parameter $T_0 = 270$ MeV has been taken over for applications in QCD with N_f quark flavors while following Ref. [45] its dependence on quark flavors and chemical potential should be invoked. Accordingly, for the case $N_f = 2 + 1$ discussed in the present work, in [45] the value $T_0 = 187$ MeV is suggested with an error margin of about 30 MeV. Applying the Matsubara formalism of finite temperature field theory, the squared quark 4-momenta are to be replaced by $(p_n^\alpha)^2 = (\omega_n^\alpha)^2 + \vec{p}^2$,

$\omega_n^\alpha = \omega_n + \alpha\phi_3$, where $\omega_n = (2n+1)\pi T$ are the fermionic Matsubara frequencies and the indices $\alpha = -1, 0, +1$ specify the three quark colors and their coupling to the parameter ϕ_3 of the temporal gauge field. At vanishing chemical potential, the Polyakov loop is given by

$$\begin{aligned} \Phi = \bar{\Phi} &= \frac{1}{N_c} \left(1 + e^{i\frac{\phi_3}{T}} + e^{-i\frac{\phi_3}{T}} \right) \\ &= \frac{1}{N_c} \left(1 + 2 \cos \left(\frac{\phi_3}{T} \right) \right). \end{aligned} \quad (4)$$

In order to check the sensitivity to various parameterizations of the Polyakov-loop potential, we will also try the polynomial form [17]

$$\frac{\mathcal{U}_{\text{poly}}(\Phi, \bar{\Phi})}{T^4} = -\frac{b_2(T)}{4} (|\Phi|^2 + |\bar{\Phi}|^2) - \frac{b_3}{6} (\Phi^3 + \bar{\Phi}^3) + \frac{b_4}{16} (|\Phi|^2 + |\bar{\Phi}|^2)^2 \quad (5)$$

with the temperature-dependent coefficient

$$b_2(T) = a_0 + a_1 \left(\frac{T_0}{T} \right) + a_2 \left(\frac{T_0}{T} \right)^2 + a_3 \left(\frac{T_0}{T} \right)^3 \quad (6)$$

and the the set of parameters from Ref. [17], $a_0 = 6.75$, $a_1 = -1.95$, $a_2 = 2.625$, $a_3 = -7.44$, $b_3 = 0.75$, and $b_4 = 7.5$.

For the effective gluon propagator in a Feynman-like gauge, $g^2 D_{\mu\nu}^{\text{eff}}(p-q) = \delta_{\mu\nu} D(p^2, q^2, p \cdot q)$, we employ a rank-2 separable ansatz [42]

$$\begin{aligned} D(p^2, q^2, p \cdot q) &= D_0 \mathcal{F}_0(p^2) \mathcal{F}_0(q^2) \\ &+ D_1 \mathcal{F}_1(p^2) (p \cdot q) \mathcal{F}_1(q^2), \end{aligned} \quad (7)$$

so that the quark propagator amplitudes are given by

$$B_f((p_n^\alpha)^2, T) = m_f^0 + b_f(T) \mathcal{F}_0((p_n^\alpha)^2), \quad (8)$$

$$A_f((p_n^\alpha)^2, T) = 1 + a_f(T) \mathcal{F}_1((p_n^\alpha)^2), \quad (9)$$

$$C_f((p_n^\alpha)^2, T) = 1 + c_f(T) \mathcal{F}_1((p_n^\alpha)^2), \quad (10)$$

and their analytic properties are defined by the choice of the form factors. In the present work we will use the

functions [51, 52]

$$\mathcal{F}_0(p^2) = \exp(-p^2/\Lambda_0^2), \quad (11)$$

$$\mathcal{F}_1(p^2) = \frac{1 + \exp(-p_0^2/\Lambda_1^2)}{1 + \exp((p^2 - p_0^2)/\Lambda_1^2)}, \quad (12)$$

which satisfy the constraints $\mathcal{F}_0(0) = \mathcal{F}_1(0) = 1$ and $\mathcal{F}_0(\infty) = \mathcal{F}_1(\infty) = 0$. Their functional form can be chosen such that the 4-momentum dependence of the dynamical mass function $M(p) = B(p)/A(p)$ and the the wave function renormalization $Z(p) = 1/A(p)$ is in good agreement [29] with LQCD simulations of the quark propagator [28]. Models which employ a rank-1 separable ansatz (see, e.g., [25, 27]) result in $A(p) = Z(p) = 1$ and miss an important aspect of quark dynamics in QCD.

The temperature-dependent gap functions $a_f(T)$, $b_f(T)$ and $c_f(T)$ are obtained as solutions of the DSE for the quark self energy in rainbow-ladder truncation as [42]

$$a_f(T) = \frac{8D_1}{27} T \sum_{n,\alpha} \int \frac{d^3p}{(2\pi)^3} \mathcal{F}_1((p_n^\alpha)^2) \bar{p}^2 A_f((p_n^\alpha)^2, T) d_f^{-1}((p_n^\alpha)^2, T), \quad (13)$$

$$c_f(T) = \frac{8D_1}{9} T \sum_{n,\alpha} \int \frac{d^3p}{(2\pi)^3} \mathcal{F}_1((p_n^\alpha)^2) (\omega_n^\alpha)^2 C_f((p_n^\alpha)^2, T) d_f^{-1}((p_n^\alpha)^2, T), \quad (14)$$

$$b_f(T) = \frac{16D_0}{9} T \sum_{n,\alpha} \int \frac{d^3p}{(2\pi)^3} \mathcal{F}_0((p_n^\alpha)^2) B_f((p_n^\alpha)^2, T) d_f^{-1}((p_n^\alpha)^2, T), \quad (15)$$

where the denominator function is $d_f((p_n^\alpha)^2, T) = \bar{p}^2 A_f^2((p_n^\alpha)^2, T) + (\omega_n^\alpha)^2 C_f^2((p_n^\alpha)^2, T) + B_f^2((p_n^\alpha)^2, T)$. Eqs. (13)-(15) correspond to minima of the thermodynamical potential (1) with respect to a variation of the temperature dependent gap functions $a_f(T)$, $b_f(T)$, $c_f(T)$ and have to be supplemented by a corresponding gap equation for the Polyakov loop which follows from the extremum condition $\partial\Omega/\partial\Phi|_{\min} = 0$. Once the gap equations are solved for different temperatures, one can extract the pseudocritical temperatures for chiral and deconfinement transitions from the peak positions of the temperature derivatives of the corresponding order parameters, the quark mass functions $m_f(T) = [m_f^0 + b(T)]/[1 + a_f(T)]$ and the Polyakov loop

$\Phi(T)$, respectively. For a discussion of the quark mass function as an order parameter of the chiral transition see, e.g., Refs. [53–55].

B. Pion, kaon and sigma meson at finite temperature

At $T = 0$ the mass-shell condition for a meson as a $q\bar{q}'$ bound state of the Bethe-Salpeter equation (BSE) is equivalent to the appearance of a pole in the $q\bar{q}'$ scattering amplitude as a function of P^2 . The $q\bar{q}'$ meson Bethe-Salpeter bound-state vertex $\Gamma_{ff'}(p, P)$ is the solution of the BSE

$$-\lambda(P^2)\Gamma_{ff'}(p, P) = \frac{4}{3} \int \frac{d^4\ell}{(2\pi)^4} g^2 D_{\mu\nu}^{\text{eff}}(p - \ell) \gamma_\mu S_f(\ell_+) \Gamma_{ff'}(\ell, P) S_{f'}(\ell_-) \gamma_\nu, \quad (16)$$

where the index f (or f') stands for the quark (or antiquark) flavor (u, d or s), P is the total 4-momentum, and $\ell_\pm = \ell \pm P/2$. The meson mass is identified from $\lambda(P^2 = -M^2) = 1$.

For example, with the separable interaction, the allowed form of the solution of Eq. (16) for the pseudoscalar Bethe-Salpeter amplitude is

$$\Gamma_P(\ell; P) = \gamma_5 (iE_P(P^2) + \not{P}F_P(P^2)) \mathcal{F}_0(\ell^2). \quad (17)$$

For scalar mesons we will use a truncated form of the Bethe-Salpeter amplitude (i.e. we take only the dominant contribution)

$$\Gamma_S(\ell; P) = E_S(P^2) \mathcal{F}_0(\ell^2). \quad (18)$$

At $T \neq 0$ in the Matsubara formalism, the $O(4)$ symmetry is broken by the heat bath and we have $P \rightarrow P_m = (\nu_m, \vec{P})$ where $\nu_m = 2m\pi T$. Bound states and the poles they generate in propagators may be investi-

gated through polarization tensors, correlators, or Bethe-Salpeter eigenvalues. This pole structure is characterized by information at discrete points ν_m on the imaginary energy axis and at a continuum of 3-momenta. One may search for poles as a function of \vec{P}^2 thus identifying the so-called spatial or screening masses for each Matsubara mode. These serve as one particular characterization of the propagator and the $T > 0$ bound states. In the present context, the eigenvalues of the BSE become $\lambda(P^2) \rightarrow \tilde{\lambda}(\nu_m^2, \vec{P}^2; T)$. The spatial screening masses are identified by zeros of $1 - \tilde{\lambda}(0, \vec{P}^2; T)$.

The general form of the finite- T pseudoscalar and scalar Bethe-Salpeter amplitude allowed by the separable model for the lowest Matsubara mode $\nu_0 = 0$ (as required for the spatial meson modes of interest here) is

$$\begin{aligned} \Gamma_P(\ell_n^\alpha; \vec{P}) &= \gamma_5 \left(iE_P(\vec{P}^2) + \vec{\gamma} \cdot \vec{P} F_P(\vec{P}^2) \right) \mathcal{F}_0((\ell_n^\alpha)^2) \\ \Gamma_S(\ell_n^\alpha; \vec{P}) &= E_S(\vec{P}^2) \mathcal{F}_0((\ell_n^\alpha)^2) \end{aligned} \quad (19)$$

One can then write the BSE for the spatial masses as

$$\tilde{\lambda}(0, \vec{P}^2; T) \Gamma_{ff'}(p_m^\alpha; \vec{P}) = \frac{4}{9} T \sum_{n, \alpha} \int \frac{d^3 \ell}{(2\pi)^3} g^2 D_{\mu\nu}^{\text{eff}}(\omega_m^\alpha - \omega_n^\alpha, \vec{p} - \vec{\ell}) \gamma_\mu S_f((\ell_n^\alpha)_+) \Gamma_{ff'}(\ell_n^\alpha, \vec{P}) S_{f'}((\ell_n^\alpha)_-) \gamma_\nu. \quad (20)$$

For example, BSE for the scalar σ meson is

$$\begin{aligned} \tilde{\lambda}_S(0, \vec{P}^2; T) = & \frac{16D_0}{9} T \sum_{n, \alpha} \int \frac{d^3 \ell}{(2\pi)^3} \mathcal{F}_0^2((\ell_n^\alpha)^2) [(\omega_n^\alpha)^2 \sigma_{C,u}((\ell_n^\alpha)_+) \sigma_{C,u}((\ell_n^\alpha)_-) \\ & + \left(\vec{\ell}^2 - \frac{\vec{P}^2}{4} \right) \sigma_{A,u}((\ell_n^\alpha)_+) \sigma_{A,u}((\ell_n^\alpha)_-) - \sigma_{B,u}((\ell_n^\alpha)_+) \sigma_{B,u}((\ell_n^\alpha)_-)] , \end{aligned} \quad (21)$$

where $\sigma_{A,f} = A_f/d_f$, $\sigma_{C,f} = C_f/d_f$ and $\sigma_{B,f} = B_f/d_f$. Further details on the analysis of mesonic spatial screening masses in other channels and for specific model interaction kernels can be found, e.g., in Ref. [42, 51, 52]. Here, we have generalized this approach by accounting for the PL phase factors entering the quark propagators and the interaction kernels.

III. RESULTS AND DISCUSSION

For the numerical calculations we fix the free parameters of the model at $T = 0$ as in Refs. [51, 52, 58], to reproduce in particular the vacuum masses of the pseudoscalar and vector mesons, $M_\pi = 140$ MeV, $M_K = 495$ MeV, $M_\rho = 770$ MeV, the pion decay constant $f_\pi = 92$ MeV, and decay widths, $\Gamma_{\rho^0 \rightarrow e^+e^-} = 6.77$ keV, $\Gamma_{\rho \rightarrow \pi\pi} = 151$ MeV as basic requirements from low-energy QCD phenomenology.

For clarity we point out that at $T = 0$, the model without PL coincides with the otherwise same model including PL (just as they do in the NJL vs. PNJL case). We thus obtain the same parameter set as in Refs. [51, 52, 58], namely $m_u^0 = m_d^0 = m_q^0 = 5.49$ MeV, $m_s^0 = 115$ MeV, $D_0 \Lambda_0^2 = 219$, $D_1 \Lambda_0^4 = 69$, $\Lambda_0 = 0.758$ GeV, $\Lambda_1 = 0.961$ GeV and $p_0 = 0.6$ GeV.

A. Order parameters for chiral and deconfinement transition

In Fig. 1 we show the resulting temperature dependence of the derivatives of the quark mass being an order parameter of the chiral phase transition and of the Polyakov loop expectation value as an order parameter of the deconfinement transition. The peak values are attained at the corresponding pseudocritical temperatures for the chiral (T_χ) and deconfinement (T_d) transitions,

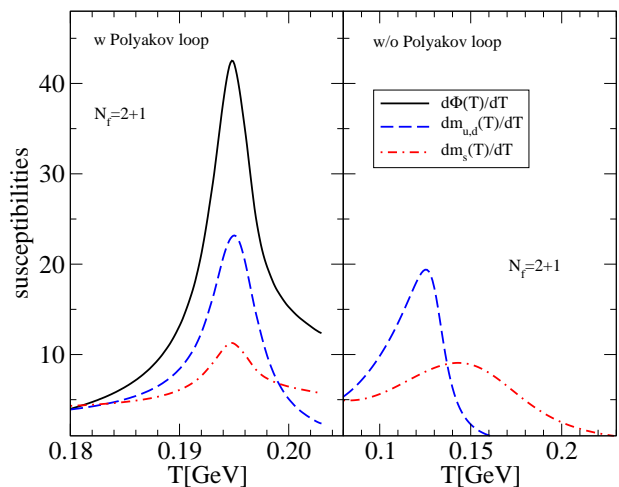


FIG. 1: (Color online) Quark mass susceptibilities (blue dashed line: light flavors; red dash-dotted line: strange flavor) with coupling to the Polyakov loop (left panel) and without it (right panel) as a function of the temperature. Note that without coupling to the Polyakov loop the chiral transition temperature is unrealistically low and the peak value for the light flavors is different from that for the strange one.

respectively. In the right panel of Fig. 1 we show the results when the quark and gluon sectors are uncoupled. In this case we have in the light quark sector $T_\chi = 128$ MeV, whereas $T_d = 270$ MeV according to the parametrization of the PL potential in the pure gauge sector. The value obtained for T_χ is in the typical range found in the DSE approach [41]. The peak position of the chiral susceptibility in the strange quark sector does not coincide with the one in the light quark sector in this case. When the quark and gluon sectors are coupled these temperatures get synchronized so that $T_c = T_\chi = T_d = 195$ MeV, as is demonstrated in the left panel of Fig. 1.

At the same time, when coupling the PL potential to

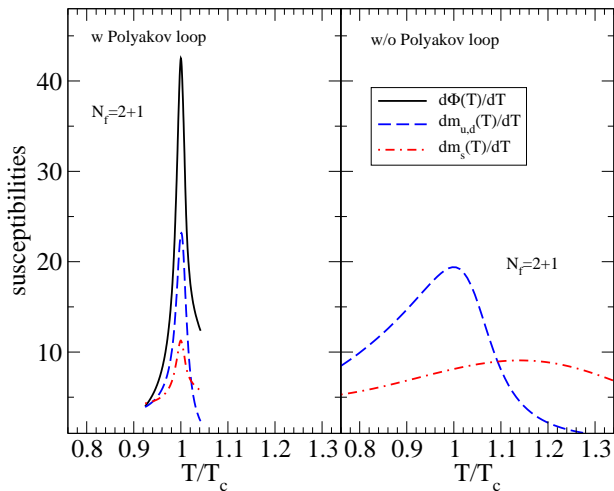


FIG. 2: (Color online) Same as Fig. 1, but as a function of the scaled temperature T/T_c with $T_c = 195$ MeV (left panel) and $T_c = T_\chi = 128$ MeV (right panel). Without coupling to the Polyakov-loop $T_d = 2.11 T_c$ is outside the range shown.

the chiral quark sector, the width of the transition region collapses to a tiny temperature interval around T_c , as is demonstrated in Fig. 2 where the susceptibilities are shown as functions of the scaled temperature T/T_c in the same interval with (left panel) and without (right panel) coupling the quark sector to the Polyakov loop potential.

Both effects of coupling the chiral quark sector to the PL, the synchronization of the chiral and deconfinement transitions as well as the narrowing of the width of the QCD transition region, are obtained in a similar way for the polynomial PL potential (5).

The value obtained for the QCD transition temperature, $T_c = 195$ MeV (193 MeV) for the logarithmic (polynomial) PL potential, is closer to recent LQCD results than the one obtained in PNJL or rank-1 separable non-local PNJL models but unsatisfactory for a quantitative description. Within the framework of the PQM model, it has been suggested [45] to rescale the T_0 parameter of the PL potential depending on the quark flavor content of the system and the chemical potential. We will follow such a prescription also in the present approach. In Fig. 3, we show the resulting temperature dependence of the order parameters for chiral symmetry breaking (the normalized mass function $m(T)/m(0)$) and for deconfinement (the PL $\Phi(T)$) for three values of T_0 . According to [45] the case $T_0 = 187$ MeV corresponds to $N_f = 2 + 1$ while $T_0 = 270$ MeV is the value for the pure gauge theory where the deconfinement is a first order phase transition. The coupling to the chiral quark dynamics changes the character of this transition to a crossover. Lowering the T_0 parameter to 187 MeV changes both deconfinement and chiral restoration to strong first order phase transitions! This change of character happens at the critical value $T_0 = 210$ MeV, also shown in Fig. 3.

In Fig. 4, we summarize this finding by showing the dependence of T_c on the T_0 parameter of the PL po-

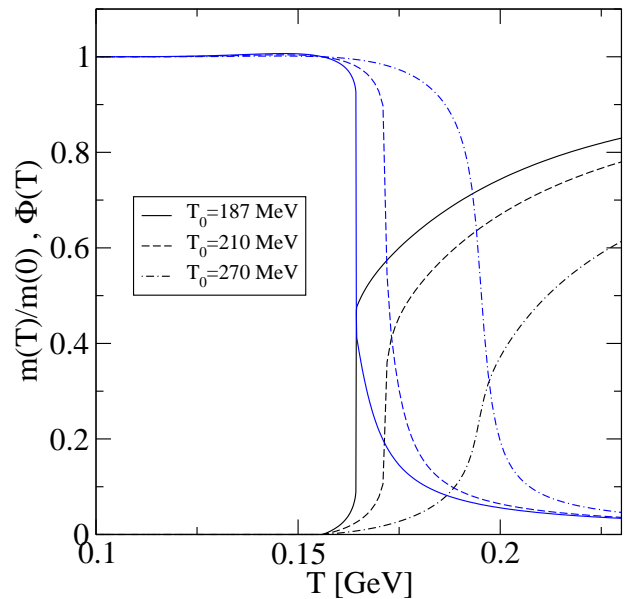


FIG. 3: (Color online) Temperature dependence of the order parameters for chiral symmetry breaking ($m(T)/m(0)$, blue lines) and for deconfinement ($\Phi(T)$, black lines) for different choices for the parameter T_0 in the Polyakov-loop potential.

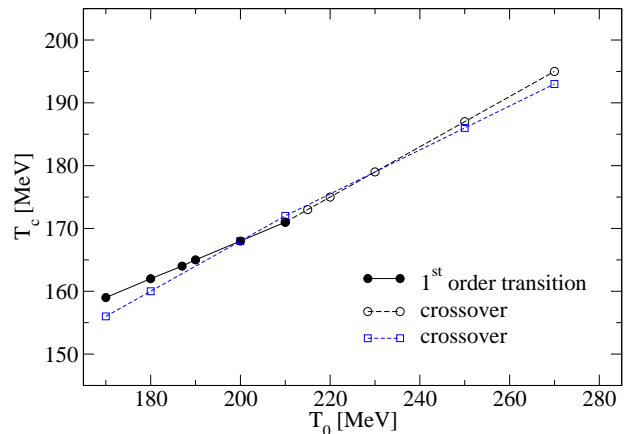


FIG. 4: (Color online) Pseudocritical temperature for the chiral restoration transition vs. parameter T_0 of the Polyakov-loop potential in the logarithmic form (3) (black circles) and in the polynomial form (5) (blue squares). For further details, see text.

tentials (3) and (5). For the logarithmic PL potential (3), the positions of first order transitions are characterized by the full dots connected by a solid line, while the crossover transitions are given as open dots connected by a dashed line. Two regions of linear dependence can be identified when using the logarithmic PL potential: $T_c = \text{const} + 0.30 T_0$ for $T_0 < 210$ MeV and $T_c = \text{const} + 0.40 T_0$ for $T_0 > 210$ MeV. When using the polynomial form (5) of the PL potential, we find the linear dependence as $T_c = \text{const} + 0.36 T_0$. The change in the character of the QCD transition from a crossover for

$T_0 > 210$ MeV to a first order transition for $T_0 < 210$ MeV is accompanied by a sudden change in slope at $T_0 = 210$ MeV. It is remarkable that the T_0 -rescaling introduced to account for a quark flavor dependence of the PL potential when applied to the nonlocal separable PDSE model considered here, results in an obvious contradiction with LQCD concerning the character of the QCD transition: while in LQCD for $N_f = 2 + 1$ the finite-T transition is a crossover [56, 57], the application of the suggested reparametrization with the corresponding value $T_0 = 187$ MeV leads in the present model to a first order transition.

On the other hand, for the polynomial PL potential (5) the transition is a crossover for any of the considered values of T_0 . Fig. 4 illustrates this by the dashed line connecting the points depicted by squares.

B. Meson screening masses at finite T

Following the approach to spatial meson screening masses developed in [42] in its generalization by the coupling to the Polyakov loop as given above, we have evaluated the temperature dependence of scalar and pseudoscalar meson masses. In Fig. 5, we show the results with (lower panel) and without (upper panel) PL coupling together with the behavior of the threshold to the continuum estimated by the sum of the corresponding quark mass functions. Since the PL coupling leads to a strong suppression of thermal quark excitations below the critical temperature, the continuum thresholds are almost constant with a sudden drop in the vicinity of T_c . This behavior is reflected in the temperature dependence of the meson screening masses. As a quantitative measure for the width of the QCD transition, we suggest to consider either the difference of σ - and π - mass squared, $\Delta_{\sigma-\pi}^2 = M_\sigma^2 - M_\pi^2$, or the difference between the temperature $T_{\sigma-2\pi}$ where the σ meson mass equals the double pion mass (the threshold for closing the $\sigma \rightarrow 2\pi$ decay channel and the temperature $T_\sigma - 2q$ where the σ meson mass equals the double quark mass (the threshold for opening the $\sigma \rightarrow 2q$) decay channel). Both measures reveal that the width of the transition region reduces from about 10 % without to about 1 % with PL coupling. Note that our results for the temperature dependence of the σ - and π - meson without PL coupling are very similar to those obtained earlier within the DSE approach [59].

A crucial part of the correct chiral behavior of the light pseudoscalar meson octet in the DS approach, where the pseudoscalars are both $q\bar{q}$ bound states and (almost-) Goldstone bosons of the dynamically broken chiral symmetry of QCD, is the linear dependence of the squared pseudoscalar masses on the current quark masses m_q as the chiral limit is approached

$$M_P^2 = M_{ff'}^2 = \text{const} (m_f + m_{f'}). \quad (22)$$

It is therefore interesting to investigate the validity of this Gell-Mann–Oakes–Renner (GMOR)-type relationship in

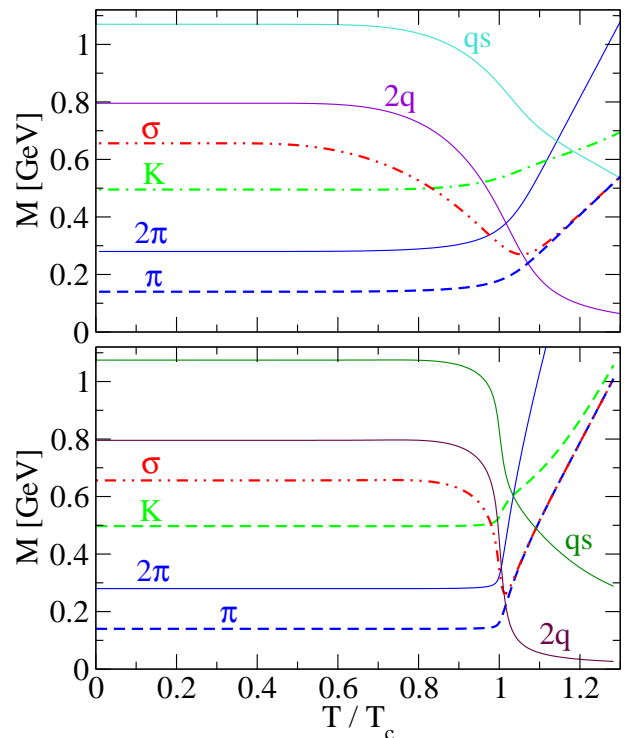


FIG. 5: Temperature dependence of pseudoscalar (π , K) and scalar (σ) meson masses in the present model without (upper panel) and with (lower panel) coupling to the Polyakov-loop potential. The temperature $T_{\sigma-2\pi}$ ($T_\sigma - 2q$) where the σ meson mass equals the double pion mass (double quark mass) determines the threshold for closing (opening) the $\sigma \rightarrow 2\pi$ ($\sigma \rightarrow 2q$) decay channel.

the present approach in the vacuum and at finite temperatures.

To this end, one calculates $M_P^2 = M_{ff'}^2$, the variable “pion” mass, for different values of current light quark mass, m_q , while the current strange quark mass is kept fixed. In Fig. 6 we show that this relation is very well fulfilled in the vacuum ($T = 0$) up to current quark masses well exceeding $10 m_q^0$. At finite temperatures, the GMOR-like relation (22) qualitatively holds well up to $T \sim T_c$.

From the temperature independence of the pion mass up to T_c , together with the validity of the GMOR-like relation in this range of temperatures, we can conclude that the temperature dependence of the chiral condensate must be mirrored by that of f_π^2 . It is a question of utmost importance for the phenomenology of hadronic matter whether such a statement would also hold when one goes beyond the rainbow-ladder level of description to which we restricted ourselves in the present work.

IV. CONCLUSIONS

We have employed a Polyakov-loop Dyson-Schwinger equation approach to investigate the pseudocritical tem-

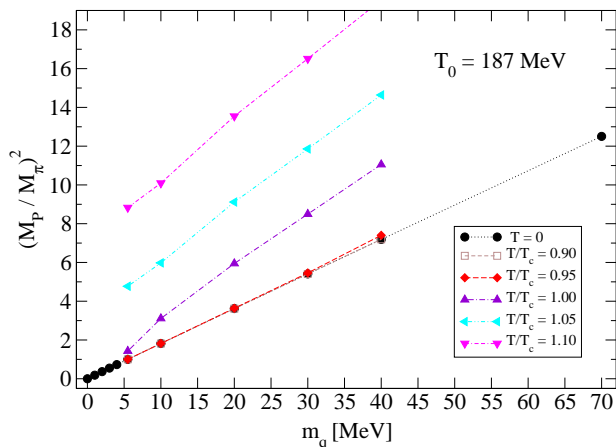


FIG. 6: Squared pseudoscalar mass vs. current quark mass for different temperatures (data symbols, connected by lines to guide the eye), show a GMOR-like behavior which holds in a wide range of quark masses, and up to temperatures very close to the critical one.

peratures for the chiral and deconfinement transitions for $N_f = 2 + 1$ quark flavors using a rank-2 separable model for the effective gluon propagator. We find that the pseudocritical temperature $T_\chi = 128$ MeV for the chiral restoration and that for deconfinement, $T_d = 270$ MeV, differ by more than a factor of two when the quark and gluon sectors are considered separately. But when the coupling is switched on these transitions get synchronized and the pseudocritical temperatures become coincident $T_c = T_\chi = T_d = 195$ MeV.

We have investigated the dependence of T_c on the parameter T_0 of the Polyakov-loop potential. For the logarithmic potential (3), we found two regions of linear dependence with a change in slope at $T_0 = 210$ MeV, accompanied with a change of the character of the QCD transition from a crossover for $T_0 > 210$ MeV to a first order transition for $T_0 < 210$ MeV. It is a remarkable finding of the present work that the T_0 -rescaling to account for a quark flavor and chemical potential dependence of the PL potential, which was suggested in [45] and investigated in greater detail in [46] for different parameterizations of the PL potential, when applied to the nonlocal separable PDSE model considered here, results in an obvious contradiction with LQCD concerning the character of the QCD transition. While in LQCD for $N_f = 2 + 1$ the finite-T transition is a crossover, in the present model with $T_0 = 187$ MeV it is a first order transition. Nevertheless, for a different form of the PL potential, namely the polynomial form (5), we find that the QCD transition remains crossover even for the smallest considered values of T_0 .

As a consequence for possible phenomenological applications of the presented approach we discussed that the coupling of the Polyakov-loop to the chiral quark dynamics narrows the temperature region in which chiral symmetry is approached. Quantitative measures for this

region are the σ - π squared mass difference ($M_\sigma^2 - M_\pi^2$) and the difference of temperatures for opening the $\sigma \rightarrow \bar{q}q$ decay channel ($T_{\sigma \rightarrow \bar{q}q}$) and the closing of the $\sigma \rightarrow 2\pi$ decay ($T_{\sigma \rightarrow 2\pi}$).

The narrowness of the QCD transition region ($\Delta T/T_c$) obtained from these measures is at the one-percent level and thus much too small for an adequate description of the QCD transition as obtained in recent LQCD studies (see, e.g., Ref. [60]).

We conclude that the separable PDSE approach provides an essential improvement of the chiral quark dynamics in PNJL models and nonlocal PNJL models which use a rank-1 separable ansatz for the quark interaction kernel, since it provides a running of both, the dynamical quark-mass function and the wave-function renormalization in close agreement with LQCD simulations of the quark propagator. It also provides the strong-coupling aspect of a dynamical confinement mechanism due to the absence of real quark mass poles.

However, the investigation of the temperature dependence of the chiral and deconfinement order parameters characterizing the (pseudo-)critical temperature and the width of the QCD transition reveals also some inadequate aspects of the present level of description of this transition. The critical temperature is too high and the transition region is too narrow when compared with LQCD results. A rescaling of the PL-potential results in a lower value for T_c , in accordance with recent LQCD results, but at the price of a narrowing of the QCD transition region, for the logarithmic PL potential even changing the character of the transition to a first order one, in striking contradiction with LQCD.

We expect that going beyond the rainbow-ladder level by including hadronic fluctuations beyond the mean field [47, 61, 63] will entail an improvement of the approach. As has been demonstrated recently by including π and σ fluctuations in a consistent $1/N_c$ scheme [62, 63], going beyond the mean field will lead to a lowering of the chiral transition temperature. The width of the transition region, however, appears as a sensitive constraint for the choice of an appropriate functional form of the PL potential. Its possible dependence on the inclusion of hadronic correlations deserves a detailed study. We plan to extend our work in this direction.

Acknowledgments

We thank R. Alkofer, S. Benić, M. Blank, K.A. Bugaev, H. Gies, Yu.L. Kalinovsky, A. Krasnigg, J.M. Pawłowski, A.E. Radzhabov, K. Redlich and B.-J. Schaefer for their discussions and comments to this paper. D.H. is grateful for and acknowledges that these materials are based on work financed with support from the National Foundation for Science, Higher Education and Technological Development of the Republic of Croatia. D.K. acknowledges the partial support of Abdus Salam ICTP. D.H. and D.K. also acknowledge the support of the

project No. 119-0982930-1016 of the Ministry of Science, Education and Sports of Croatia. D.B. was supported by the Russian Foundation for Basic Research under grant No. 08-02-01003-a and by the Polish Ministry of Science and Higher Education (MNiSW) under

grant No. NN 202 2318 37. This work was supported in part by CompStar, a Research Networking Programme of the European Science Foundation and by the Polish MNiSW grant "COMPSTAR-POL" No. 790/N-RNP-COMPSTAR/2010/0.

-
- [1] Y. Aoki, S. Borsanyi, S. Durr, Z. Fodor, S. D. Katz, S. Krieg and K. K. Szabo, *JHEP* **0906**, 088 (2009).
- [2] S. Borsanyi, Z. Fodor, C. Hoelbling, S. D. Katz, S. Krieg, C. Ratti and K. K. Szabo, *JHEP* **1009**, 073 (2010).
- [3] S. Borsanyi *et al.*, *JHEP* **1011**, 077 (2010).
- [4] M. Cheng *et al.*, *Phys. Rev. D* **81**, 054504 (2010).
- [5] A. Bazavov and P. Petreczky, *J. Phys. Conf. Ser.* **230**, 012014 (2010).
- [6] A. Bazavov and P. Petreczky, arXiv:1009.4914 [hep-lat].
- [7] A. Bazavov and P. Petreczky, *PoS LATTICE2010*, 169 (2010).
- [8] W. Söldner [HotQCD collaboration], *PoS LATTICE2010*, 215 (2010).
- [9] P. Braun-Munzinger, K. Redlich and J. Stachel, arXiv:nucl-th/0304013.
- [10] P. Braun-Munzinger, D. Magestro, K. Redlich and J. Stachel, *Phys. Lett. B* **518**, 41 (2001).
- [11] Y. Nambu and G. Jona-Lasinio, *Phys. Rev.* **122**, 345 (1961); **124**, 246 (1961).
- [12] M. K. Volkov, *Annals Phys.* **157**, 282 (1984); *Sov. J. Part. Nucl.* **17**, 186 (1986).
- [13] S. Klimt, M. Lutz, U. Vogl and W. Weise, *Nucl. Phys. A* **516**, 429 (1990); *Nucl. Phys. A* **516**, 469 (1990).
- [14] S. P. Klevansky, *Rev. Mod. Phys.* **64**, 649 (1992).
- [15] T. Hatsuda and T. Kunihiro, *Phys. Rept.* **247**, 221 (1994).
- [16] M. Buballa, *Phys. Rept.* **407**, 205 (2005).
- [17] C. Ratti, M. A. Thaler and W. Weise, *Phys. Rev. D* **73**, 014019 (2006).
- [18] P. N. Meisinger and M. C. Ogilvie, *Phys. Lett. B* **379**, 163 (1996).
- [19] K. Fukushima, *Phys. Lett. B* **591**, 277 (2004).
- [20] E. Megias, E. Ruiz Arriola and L. L. Salcedo, *Phys. Rev. D* **74**, 114014 (2006).
- [21] C. Sasaki, B. Friman and K. Redlich, *Phys. Rev. D* **75**, 074013 (2007).
- [22] C. Ratti, S. Roessner and W. Weise, *Phys. Lett. B* **649**, 57 (2007).
- [23] Y. Sakai, K. Kashiwa, M. Matsuzaki, H. Kuono and M. Yahiro, *Phys. Rev. D* **79**, 096001 (2009).
- [24] Y. Sakai, T. Sasaki, H. Kuono and M. Yahiro, *Phys. Rev. D* **82**, 076003 (2010).
- [25] D. Blaschke, M. Buballa, A. E. Radzhabov and M. K. Volkov, *Yad. Fiz.* **71**, 2012 (2008) [*Phys. Atom. Nucl.* **71**, 1981 (2008)].
- [26] G. A. Contrera, D. Gomez Dumm and N. N. Scoccola, *Phys. Lett. B* **661**, 113 (2008).
- [27] T. Hell, S. Roessner, M. Cristoforetti and W. Weise, *Phys. Rev. D* **79**, 014022 (2009).
- [28] M. B. Parappilly, P. O. Bowman, U. M. Heller, D. B. Leinweber, A. G. Williams and J. B. Zhang, *Phys. Rev. D* **73**, 054504 (2006).
- [29] S. Noguera and N. N. Scoccola, *Phys. Rev. D* **78**, 114002 (2008).
- [30] G. A. Contrera, M. Orsaria and N. N. Scoccola, *Phys. Rev. D* **82**, 054026 (2010).
- [31] R. Alkofer and L. von Smekal, *Phys. Rept.* **353**, 281 (2001).
- [32] C. D. Roberts and S. M. Schmidt, *Prog. Part. Nucl. Phys.* **45**, S1 (2000).
- [33] C. S. Fischer, *J. Phys. G* **32**, R253 (2006).
- [34] C. S. Fischer, *Phys. Rev. Lett.* **103**, 052003 (2009).
- [35] C. S. Fischer, J. A. Mueller, *Phys. Rev. D* **80**, 074029 (2009).
- [36] K. I. Kondo, *Phys. Rev. D* **82**, 065024 (2010).
- [37] J. Braun, H. Gies and J. M. Pawłowski, *Phys. Lett. B* **684**, 262 (2010).
- [38] J. Braun, L. M. Haas, F. Marhauser, J. M. Pawłowski, *Phys. Rev. Lett.* **106**, 022002 (2011).
- [39] J. Braun and A. Janot, arXiv:1102.4841 [hep-ph]
- [40] R. Alkofer, *PoS FACESQCD*, 030 (2011).
- [41] M. Blank and A. Krassnigg, *Phys. Rev. D* **82**, 034006 (2010).
- [42] D. Blaschke, G. Bureau, Yu. L. Kalinovsky, P. Maris and P. C. Tandy, *Int. J. Mod. Phys. A* **16**, 2267 (2001).
- [43] C. J. Burden, L. Qian, C. D. Roberts, P. C. Tandy and M. J. Thomson, *Phys. Rev. C* **55**, 2649 (1997).
- [44] J. Braun and H. Gies, *Phys. Lett. B* **645**, 53 (2007).
- [45] B. J. Schaefer, J. M. Pawłowski and J. Wambach, *Phys. Rev. D* **76**, 074023 (2007).
- [46] B. J. Schaefer, M. Wagner and J. Wambach, *Phys. Rev. D* **81**, 074013 (2010).
- [47] T. K. Herbst, J. M. Pawłowski and B. J. Schaefer, *Phys. Lett. B* **696**, 58 (2011).
- [48] J. M. Cornwall, R. Jackiw and E. Tomboulis, *Phys. Rev. D* **10**, 2428 (1974).
- [49] R. W. Haymaker, *Riv. Nuov. Cim.* **14** (1991).
- [50] S. Rößner, C. Ratti and W. Weise, *Phys. Rev. D* **75**, 034007 (2007).
- [51] D. Blaschke, D. Horvatic, D. Klabucar and A. E. Radzhabov, arXiv:hep-ph/0703188.
- [52] D. Horvatic, D. Blaschke, D. Klabucar and A. E. Radzhabov, *Phys. Part. Nucl.* **39**, 1033 (2008).
- [53] A. Bender, D. Blaschke, Y. Kalinovsky and C. D. Roberts, *Phys. Rev. Lett.* **77**, 3724 (1996).
- [54] D. Blaschke, A. Höll, C. D. Roberts and S. M. Schmidt, *Phys. Rev. C* **58**, 1758 (1998).
- [55] A. Höll, P. Maris and C. D. Roberts, *Phys. Rev. C* **59**, 1751 (1999).
- [56] Y. Aoki, G. Endrodi, Z. Fodor, S. D. Katz and K. K. Szabo, *Nature* **443**, 675 (2006).
- [57] S. Ejiri *et al.*, *Phys. Rev. D* **80**, 094505 (2009).
- [58] D. Blaschke, Y. L. Kalinovsky, A. E. Radzhabov and M. K. Volkov, *Phys. Part. Nucl. Lett.* **3**, 327 (2006).
- [59] P. Maris, C. D. Roberts, S. M. Schmidt and P. C. Tandy, *Phys. Rev. C* **63**, 025202 (2001).
- [60] M. Cheng *et al.*, *Eur. Phys. J. C* **71**, 1564 (2011).
- [61] V. Skokov, B. Stokic, B. Friman and K. Redlich, *Phys.*

- Rev. C **82**, 015206 (2010).
- [62] D. Blaschke, M. Buballa, A. E. Radzhabov and M. K. Volkov, Nucl. Phys. Proc. Suppl. **198**, 51 (2010).
- [63] A. E. Radzhabov, D. Blaschke, M. Buballa and M. K. Volkov, Phys. Rev. C **83**, 116004 (2011).